Fibers and Polymers 2022, Vol.23, No.6, 1582-1594
DOI 10.1007/s12221-022-4992-4

ISSN 1229-9197 (print version)
ISSN 1875-0052 (electronic version)

Nanoparticle-free, Fluorine-free, and Robust Superhydrophobic Cotton Fabric Fabricated Using a Combination of Etching Method and Mist Polymerization Technology

Qingbo Xu[1]*, Xinyu Wang[1], Wei Xu[2], YanYan Zhang[1], and Zhenzhen Xu[1]*

[1]*Key Laboratory of Textile Fabric, College of Textiles and Clothing, Anhui Polytechnic University, Wuhu, Anhui 241000, China*
[2]*Nanchong Hospital of Traditional Chinese Medicine, Sichuan Nanchong 637000, China*
(Received September 15, 2021; Revised October 20, 2021; Accepted October 27, 2021)

Abstract: Immobilizing inorganic or organic particles on cotton fabric to increase the surface roughness, followed by coating with low surface reagents to reduce the surface energy, are the dominant strategies to prepare the superhydrophobic cotton surface. However, the inorganic or organic particles can easily fall off the surface of the fabrics. Thus, the surface roughness of the fabric could be reduced during the process, resulting in the poor durability of the superhydrophobic fabric. In this work, the surface of the cotton fabric was etched by cellulase. Following this, the treated fabric was grafted using a diblock copolymer (poly[(methyl methacrylate)-*b*-(2-(dimethylamino)ethyl)] (PMMA-*b*-PDMAEMA)), which was synthesized following the reversible addition-fragmentation chain transfer (RAFT) polymerization process. The mist polymerization technology was used for the process. The coatings successfully endowed the cotton fabric with superhydrophobic properties. The maximum WCA value recorded was 159.9 °. The treated fabric exhibited excellent mechanical and chemical stability. Moreover, the modified cotton sample also exhibited good self-cleaning effects in the presence of solid dust and liquid contaminants. It also exhibited excellent oil-water separation properties. Therefore, the superhydrophobic fabric prepared using a combination of the etching method and mist polymerization technology can find its potential application in home and industrial areas.

Keywords: Etching method, Mist polymerization, Superhydrophobic cotton fabric, Self-cleaning, Oil-water separation

Introduction

Cotton fabric is one of the most popular textiles made of natural fibers [1-4]. With the progress of science and technology, functional textiles have been widely studied and analyzed. At present, antibacterial cotton fabric [5,6], ultraviolet-visible (UV) protective cotton fabric [7-9], conductive cotton fabric [10,11], and superhydrophobic cotton fabric [12,13] have been developed to expand the application range of cotton fabric in household and industrial fields. Among these functional fabric samples, the fabric with excellent superhydrophobic properties has been used for oil-water separation in industrial areas. It has also been used for domestic purposes (for self-cleaning) [14-16].

The surface roughness needs to be improved and the surface energy needs to be reduced to obtain superhydrophobic cotton fabric [17,18]. Presently, two methods are used to improve the surface roughness of the fabric. First, inorganic particles (TiO_2 [19-21], ZnO [22-24], Ag [25], SiO_2 [26-28], and others [29,30]) or organic particles such as polystyrene microsphere [31] are immobilized on the cotton fabric to improve its surface roughness. Wang *et al*. [32] prepared nano-sized or micron-sized rod-like ZnO particles by conducting hydrothermal reactions and immobilized them on cotton fabrics. Subsequently, the surface of the treated fabric was coated with stearic acid. The aggregate structure of the ZnO particles on the fabric surface changed from loose to compact following the modification with stearic acid. As a result, the superhydrophobic fabric was obtained. The water contact angle (WCA) was recorded to be 155.0 °. Xu *et al*. [33] immobilized the fumed silica (SiO_2) particles on the fiber surface of the cotton fabric to improve surface roughness. Following this, the diblock copolymer poly[(methyl methacrylate)-*b*-(lauryl methacrylate) (PMMA-*b*-PLMA) was grafted onto the treated fabric to reduce the surface energy of the fabric. After the final coat was applied, the cotton fabric with outstanding superhydrophobic properties was obtained. The WCA value recorded was 156.7 °. The surface roughness can be increased by immobilizing inorganic or organic particles on fabric and the surface energy can be reduced by coating the fabric with low surface energy chemical reagents. This combined process can be used to successfully prepare superhydrophobic surfaces. However, the inorganic or organic particles can easily fall off the surface of the fabric, resulting in poor durability of the superhydrophobic cotton fabric.

Another method to improve the surface roughness involves the process of fabric etching using chemical or biological reagents [34-36]. Nguyen-Tri *et al*. [34] used alkali and plasma to etch cotton fabrics. Following the process of etching, the cotton fabric was coated with SiO_2 nanoparticles and tetraethyl orthosilicate (TEOS). The surface roughness of the fabric could be increased and the

*Corresponding author: xuqingbo@ahpu.edu.cn
*Corresponding author: xuzhenzhen@ahpu.edu.cn

surface energy of the fabric could be reduced. The superhydrophobic fabric was successfully prepared. The WCA value recorded was 173.0 °. The finished fabric could withstand 40 washing cycles or 30 abrasion treatments. The WCA values recorded were as high as 160.0 ° post the abrasion and washing treatment processes. Thus, excellent mechanical durability could be realized. Cheng *et al*. [37] were the first to use papain to etch silk fabric. The treated fabric was coated with methyltrichlorosilane (MTCS). The surface roughness of the fabric could be effectively improved when it was etched with papain. The experimental results indicated that the surface of the pristine fabric was smooth. The root mean square (RMS) value was 2.01 nm. However, the surface of the etched fabric was rough (RMS: >33.0 nm). In addition, the surface energy of the fabric could be reduced by coating it with MTCS. Through this modification process, the superhydrophobic fabric was manufactured. The WCA value recorded for the obtained cotton was 156.7 °. Moreover, the prepared fabric could withstand 100 abrasion treatment cycles or two accelerated washing cycles. The surface of the treated fabric exhibited superhydrophobic properties. The WCA value was recorded was 150.0 °. The value indicated that the superhydrophobic surface of the obtained fabric exhibited excellent mechanical durability. The surface roughness of the fabric can be significantly increased by etching the fabric surface. However, the mechanical strength decreased and the surface roughness reduced when low surface energy reagents were used to coat the fabric surface. Therefore, limited application of the superhydrophobic cotton is seen.

In this work, a fluorine-free diblock copolymer poly [(methyl methacrylate)-*b*-(2-(dimethylamino)ethyl)] (PMMA-*b*-PDMAEMA) was synthesized following the process of reversible addition-fragmentation chain transfer (RAFT) polymerization. Cellulose was used to etch the cotton fabric toward the end of the experiment. Significantly increased surface roughness was realized. Following this, the fiber surface of the etched fabric was grafted with PMMA-*b*-PDMAEMA following the process of transesterification using mist polymerization technology. The process resulted in reduced surface energy of the cotton fabric. The mist polymerization technology was used to graft a thin layer of the diblock copolymer PMMA-*b*-PDMAEMA onto the etched fabric surface [38-40]. The surface roughness of the diblock copolymer PMMA-*b*-PDMAEMA-grafted etched fabric could be well retained.

Experimental

Materials

The reagents including N,N-dimethylformamide (DMF), tetrahydrofuran (THF), N-hexane, chloroform, acetone, ethanol, 1,4-dioxane, methyl methacrylate (MMA), 2-(dimethylamino)ethyl methacrylate (DMAEMA), s-(Thiobenzoyl)thioglycolic acid (TA), and 2,2'-azobis(2-methylpropionitrile) (AIBN), were obtained from Shanghai Aladdin Co., Ltd. (China). The cotton fabric (60 ends/cm, 30 picks/cm, 0.42 mm thickness, 120 g/m weight, 35.2 m^2/g specific surface area) was obtained from Shaoxing Qidong Textile Co., Ltd. Before chemical modification, the cotton samples (3.0 cm×3.0 cm) were cleaned by ultrasonic washing in 1 % sodium laurylsulfonate solution for 30 min, then washing in ethanol (2 h) and deionized water (30 min× 3 times).

Synthesis Diblock Polymer of PMMA-*b*-PDMAEMA

The preparation route of the diblock copolymer PMMA-*b*-PDMAEMA by RAFT polymerization is shown in Figure 1. First, 0.17 g (8.01×10^{-4} mol) of TA, 0.13 g (8.01×10^{-4} mol) of AIBN, 8.02 g (8.01×10^{-2} mol) of MMA, and 11.90 m*l* of 1,4-dioxane were mixed in a triangular flask, deoxygenated with nitrogen gas for 30 min, heated at 90 °C for 6 h. After that, the mixtures was cooled to room temperature, added other mixture solution which included with 0.13 g (9.78×10^{-4} mol) of AIBN, 12.59 g (8.01×10^{-2} mol) of DMAEMA and 15.8 m*l* of 1,4-dioxane. The mixtures were again deoxygenated with nitrogen gas for 30 min, and reacted for 6 h at 90 °C. Finally, the product of PMMA-*b*-PDMAEMA was obtained after precipitation of the mixture in ethanol and dried at 80 °C under vacuum for 48 h.

Fabrication of Superhydrophobic Fabrics

The steps followed to synthesize PMMA-*b*-PDMAEMA used in the final stages of the fabrication process have been described in the SI.

The final stage includes three steps. The first step involves the immersion of the pristine cotton fabric (PF, 3 cm×3 cm) in a dispersion of cellulase (10 g/*l*) in an aqueous medium at

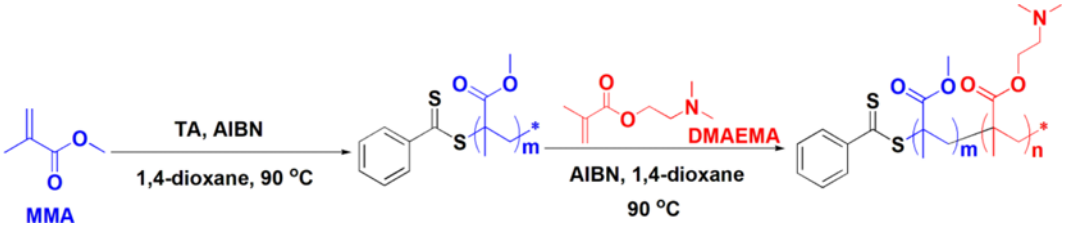

Figure 1. Synthetic route for the preparation of PMMA-*b*-PDMAEMA.

50 °C. The solution was stirred for 30 min, washed using distilled water (30 min; 3×50 m*l*), and dried at 80 °C over 2 h. The obtained fabric was labeled EF. In the second step, the solution of PMMA-*b*-PDMAEMA in acetone (1 wt.%) was atomized on one side of the EF for 5 min. The third step involves curing the treated fabric at 180 °C (curing time: 3 min). The resulting sample was laundered using acetone for 30 min (3×50 m*l*) and dried at 80 °C over 2 h to obtain SF-1. Similar steps were followed to prepare the SF-2 and SF-3 samples. However, in these cases, 2 wt.% and 3 wt.% of the acetone solution of the diblock copolymer PMMA-*b*-PDMAEMA was used, respectively.

Characterization

The characterization methods of the fabric are depicted in the Supporting Information (SI).

Results and Discussion

Structural Analysis of PMMA-*b*-PDMAEMA

The monomers MMA and DMAEMA were polymerized to synthesize PMMA-*b*-PDMAEMA via the RAFT polymerization process (Figure 1). The FTIR, ^{1}H NMR, and GPC analysis techniques were used to analyze the structure of PMMA-*b*-PDMAEMA. The functional groups present in the diblock copolymer were determined by analyzing the FTIR spectra (Figure S1). The characteristic stretching vibration peaks of the -CH_3 and -CH_2- groups appeared at 2948 cm^{-1} and 2821 cm^{-1}, respectively. The peak corresponding to the stretching vibration of C-H present in the -N$(CH_3)_2$ groups appeared at 2773 cm^{-1}. The peak at 1456 cm^{-1} was attributed to the bending vibration of the -CH_2- groups. The peak corresponding to the characteristic stretching vibration of C=O appeared at 1729 cm^{-1}. The peak at 1150 cm^{-1} was assigned to the peak corresponding to the stretching vibration of the C-O group. In addition, the characteristic peak corresponding to the C=C bond vibration was absent in the spectra, indicating that the MMA and DMAEMA monomers had completely polymerized. ^{1}H NMR spectra were recorded to further analyze the structure of PMMA-*b*-PDMAEMA, and the result is shown in Figure S2. The signal at 3.61 ppm (a, CH_3-O-) was assigned to the PMMA block. The signals at 4.07 ppm (b, $(CH_3)_2NCH_2CH_2$-), 2.59 ppm (c, $(CH_3)_2NCH_2$-), and 2.05 ppm (d, $(CH_3)_2$N-)

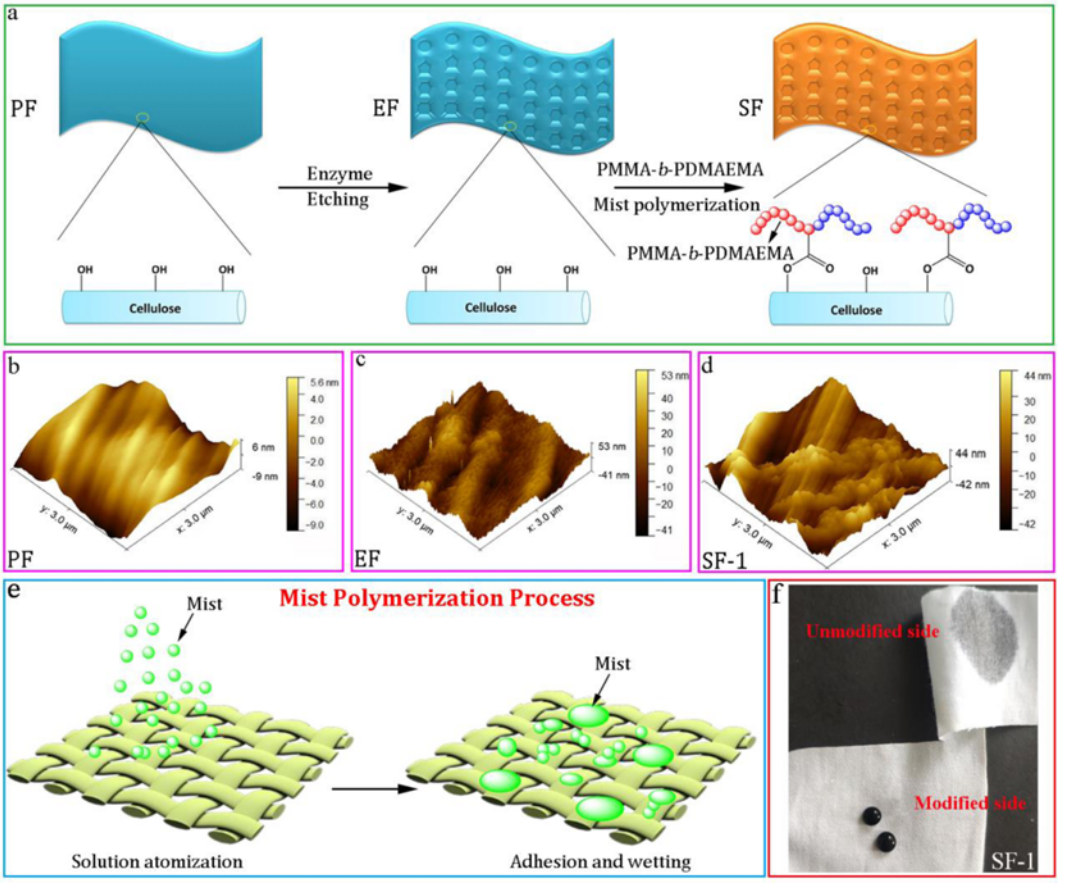

Figure 2. Synthetic route for the preparation of superhydrophobic cotton fabric (a). AFM images of PF (b), EF (c), and SF-1 (d) samples. Atomization and adhesion processes following the mist polymerization technique (e). Optical images of the SF-1 samples (f).

were attributed to the PDMAEMA block. The signals at 3.12 ppm (e, RCH_2-) and 1.88 ppm (f, RCH_2-) were assigned to the polymer chains. These results proved that the monomers of MMA and DMAEMA were successfully polymerized during the synthesis of PMMA-*b*-PDMAEMA. Figure S3 shows the GPC curves recorded for PMMA-*b*-PDMAEMA. There single peak observed in the GPC curve, corresponding to both PMMA and PDMAEMAMMA, indicated the formation of the diblock copolymer PMMA-*b*-PDMAEMA. Analysis of the GPC results revealed that the *Mn* and PDI values for the diblock copolymer were 1.8347×10^4 g/mol and 1.29, respectively. The narrow molecular weight distribution proved that the product could be successfully obtained using the RAFT polymerization technology.

Surface Structure and Morphology of the Modified Fabrics

Figure 2a shows the mechanism of formation of the superhydrophobic fabric. First, the cotton fabric was etched using an aqueous dispersion of cellulase at 50 °C (time: 30 min). This results in the roughness of the surface of the cotton fabric. Following this, the diblock copolymer PMMA-*b*-PDMAEMA was atomized on one side of the cotton fabric following the mist polymerization technique. Subsequently, it was reacted with the hydroxyl groups of the cotton fiber. The transesterification reaction was carried out. Thus, the diblock copolymer was grafted on one side of the cotton fabric, thereby exploiting covalent bonds.

The surface roughness of the cotton fabric was increased following the enzyme etching process. The surface energy was reduced by grafting the diblock copolymer PMMA-*b*-PDMAEMA. Thus, the superhydrophobic surface was successfully constructed. It is necessary to analyze the structures and properties of the modified fabric to understand the preparation mechanism.

Figures 2b-d show the AFM images of the PF, EF, and SF-1 samples. The surface of the PF sample was smooth, with the RMS value being approximately 18.6 nm (Figure 2b and Figure S4a). The surface of the EF sample appeared rough and rugged and the RMS value was 53.2 nm (Figure 2c and Figure S4b). These results indicated that the enzyme-etched fabric exhibited significantly increased surface roughness. In addition, the surface of the SF-1 sample was rough, but the degree of roughness was less than the degree of roughness observed in the EF sample (RMS: approximately 47.5 nm) (Figure 2d and Figure S4c). The results indicated that the surface roughness of the etched cotton fiber could not be significantly reduced by grafting the diblock copolymer PMMA-*b*-PDMAEMA.

The process of the mist polymerization is shown in Figure 2e. The acetone solution of the diblock copolymer PMMA-*b*-PDMAEMA was atomized using an atomizer. Then the mist of the PMMA-*b*-PDMAEMA solution was wetted and made to adhere to one side of EF. There are two advantages of using the mist polymerization technology for the fabrication of superhydrophobic surfaces. Firstly, the mist polymerization technology can be used to graft a thin layer of the diblock copolymer PMMA-*b*-PDMAEMA onto the EF surface. The surface roughness of the EF sample grafted with the diblock copolymer did not significantly reduce. Secondly, as shown in Figure 2f, the SF-1 sample prepared following the mist polymerization technology exhibits the property of double-sided anisotropy. The modified SF-1 surface exhibited excellent hydrophobic properties, while the degree of hydrophilicity of the unmodified surface was the same as the degree of hydrophilicity of PF. These results indicated that the mist polymerization technology could be used to largely maintain the surface roughness of EF. The technique can also be used to devise a flexible design for both sides of the surfaces of the fabric.

The ATR-FTIR technique was used to analyze the surface chemical groups present in the cotton fabric, and the spectra are shown in Figure 3. The characteristic bands corresponding to cellulose appeared at 3343 cm^{-1} (-OH stretching), 1429 cm^{-1} (C-H wagging), 1366 cm^{-1} (C-H bending), 1108 cm^{-1} (C-O-C, asymmetric bridge stretching), 1157 cm^{-1}, 1056 cm^{-1}, and 1031 cm^{-1} (C-O stretching) [41-46]. These bands are seen in the spectral profiles recorded with PE and the modified fabrics. The results suggested that the chemical structure of cellulose remained mostly unchanged. The spectra recorded for EF did not contain peaks that were absent in the spectra recorded for PF. This indicated that the chemical groups on the surface of the fabric remained changed post enzymatic etching. However, a new peak at 1724 cm^{-1} appeared in the spectral profiles recorded with the three modified fabric samples. It was assigned to the stretching vibration of the C=O group. This result proved that the diblock copolymer PMMA-*b*-PDMAEMA could be successfully grafted onto the surface of the EF sample.

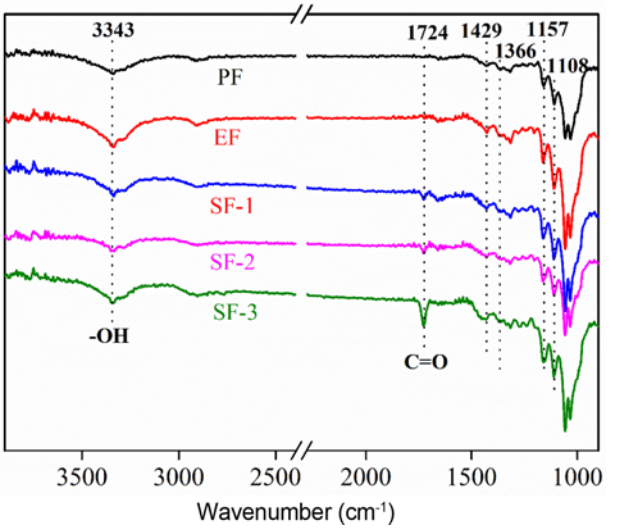

Figure 3. ATR-FTIR spectral profiles of the fabrics.

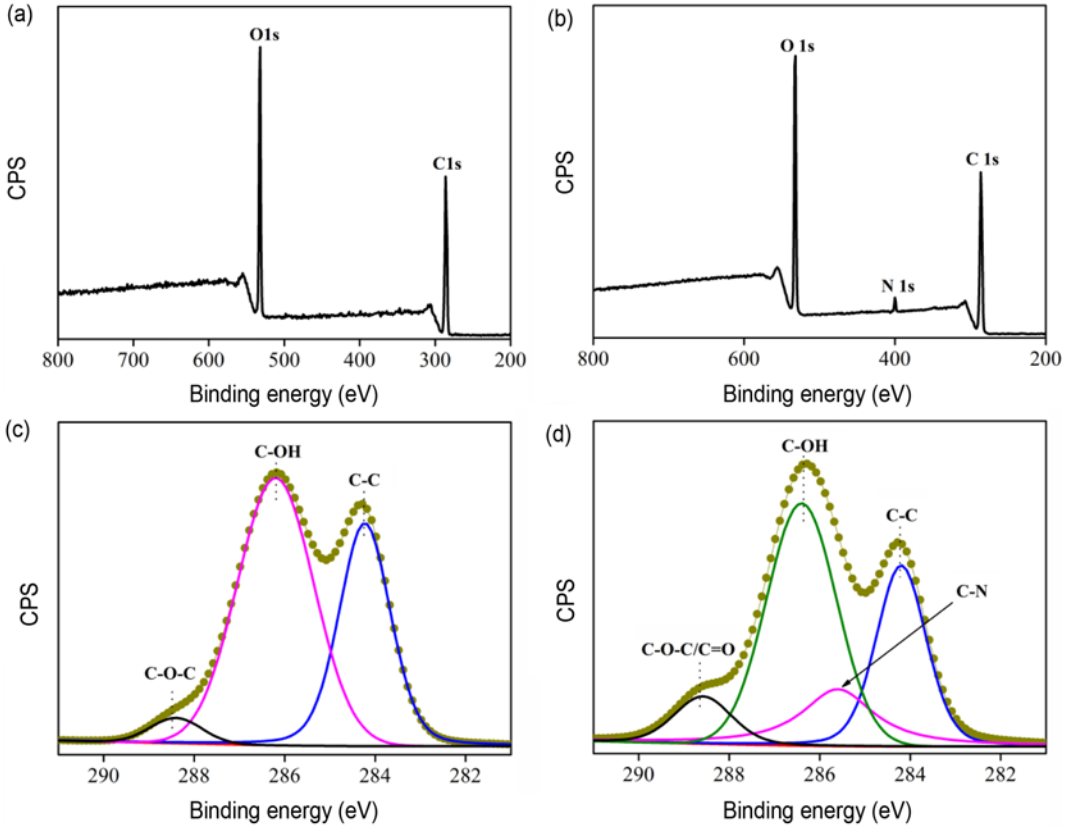

Figure 4. Wide-range XPS spectral profiles of the PF (a) and SF-1 (b) fabrics. The C 1s XPS spectral profiles of the PF (c) and SF-1 (d) samples.

Furthermore, these results demonstrated that the diblock polymer PMMA-*b*-PDMAEMA could be successfully grafted onto the cotton fabric without causing significant damage to the surface chemical structure.

Figures 4a and b show the wide-range XPS spectra of the PF and SF-1 samples. As shown in Figure 4a, the spectra recorded with the PF sample exhibits two peaks at the binding energies of 531.8 eV and 285.9 eV. These were attributed to the O 1s and C 1s signals [47,48], respectively. The spectral profile of the SF-1 sample showed an additional peak with the binding energy of 400.1 eV, which was attributed to the N 1s signal (Figure 4b) [49,50]. This result demonstrated that the diblock copolymer PMMA-*b*-PDMAEMA was present on the fabric surface.

The C 1s XPS spectral profiles of the PF and SF-1 samples are shown in Figures 4c and d. The spectral profiles recorded with PF showed the presence of peaks at 284.2 eV (C-C), 286.2 eV (C-OH), and 288.5 eV (C-O-C) [51,52]. An additional peak at 285.6 eV (C-N) [53] (absent in the spectral profile recorded with PF) was observed in the spectral profile recorded with SF-1. Moreover, the peak value of the SF-1 sample at 288.7 eV (C-O-C/C=O) did not match with that observed for the PF sample. This result indicated that the cotton fabric was successfully grafted with

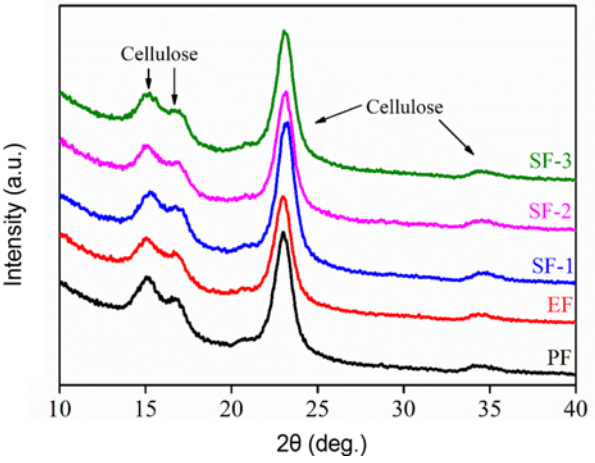

Figure 5. XRD spectral profiles of the samples.

the diblock copolymer, and new C=O bonds were formed. These results demonstrated that the diblock copolymer PMMA-*b*-PDMAEMA could be grafted onto the cotton fabric via the process of transesterification.

The XRD technique was used to study the effect of the modification process on the crystal structure of the cotton fabric. As shown in Figure 5, similar peaks at 2θ=15.1 °,

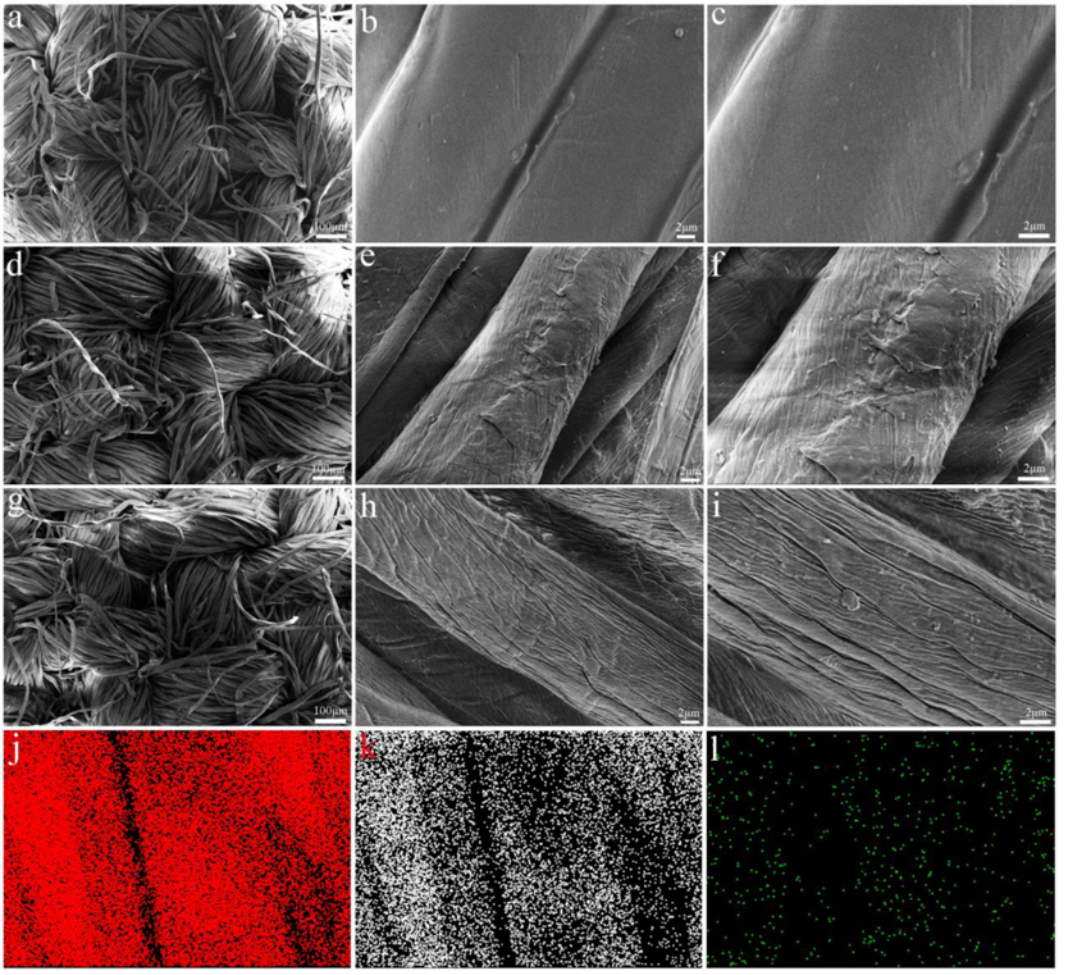

Figure 6. SEM images of the PF (a-c), EF (d-f), and SF-1 (g-i) samples. The C (j), O (k), and N (l) element mapping images of the SF-1 sample.

16.6 °, 23.0 °, and 34.6 ° appeared in the spectral profiles recorded with PF, EF, SF-1, SF-2, and SF-3, which were attributed to the cellulose (I). This result suggested that the crystal structure of the etched cotton fiber did not undergo significant damage [51,54]. The results also proved that the crystal structure of the cotton fiber was not significantly affected during the process of grafting.

The scanning electron microscopy (SEM) images of the fabric samples are shown in Figure 6 and Figure S5. Significantly different SEM images for the PF, EF, SF-1, SF-2, and SF-3 samples were not observed under conditions of low magnification. This result indicated that the etching process affects the properties of the fabric surface but does not alter the gap between the cotton fibers. The results also revealed that the diblock copolymer PMMA-*b*-PDMAEMA could be grafted onto the fiber surface without blocking the gap between the cotton fibers. Clean and smooth surfaces of the PF sample and rough and rugged surfaces of the EF, SF-1, SF-2, and SF-3 samples were observed in the SEM images recorded under conditions of high magnification. This result indicated that the surface roughness of the EF sample was effectively improved post etching, promoting the necessary conditions for the fabrication of the super-hydrophobic surfaces. In addition, this result also revealed that the surface roughness of the treated cotton fabric was not reduced to a large extent when the diblock copolymer PMMA-*b*-PDMAEMA was grafted onto the EF sample.

The carbon, oxygen, and nitrogen mapping images revealed that the diblock copolymer PMMA-*b*-PDMAEMA was evenly distributed on the surface of the SF-1 fiber. These results indicated that the surface roughness of the cotton fabrics increased following the process of etching using cellulase. The grafting of diblock copolymer PMMA-*b*-PDMAEMA using mist polymerization technology did not result in significantly reduced surface roughness of the etched cotton fabrics.

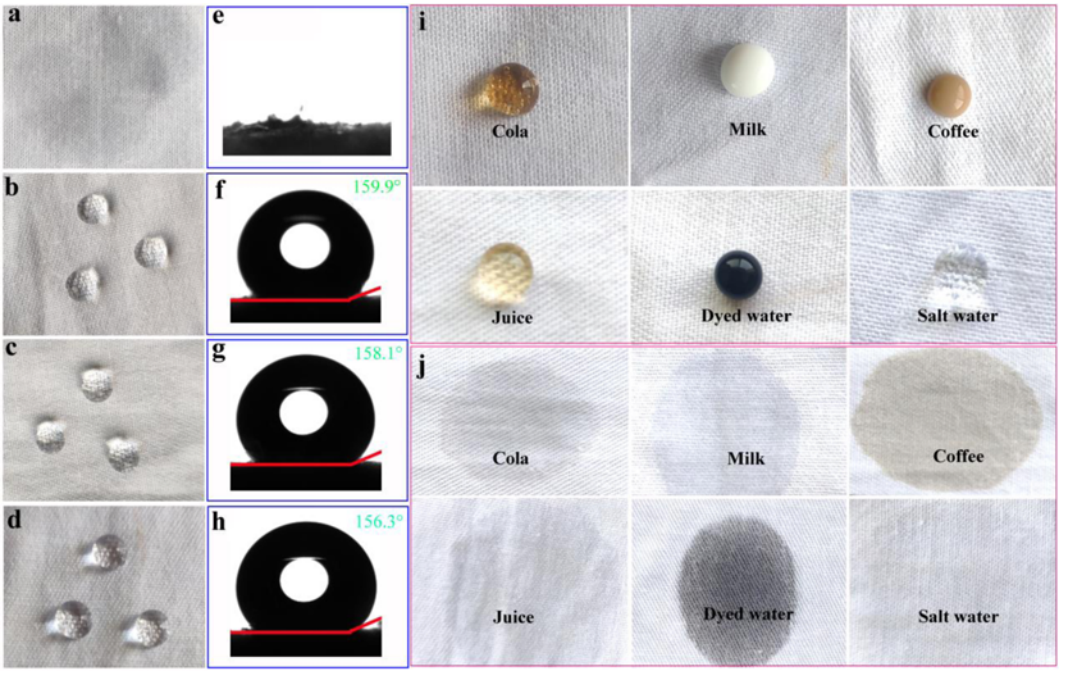

Figure 7. Image of distilled water wetted on PF (a) and placed on SF-1 (b), SF-2 (c), and SF-3 (d). WCA images of the PF (e), SF-1 (f), SF-2 (g), and SF-3 (h) samples. Optical images of several droplets placed on the surface of SF-1 (i) and wetted on the surface of PF (j).

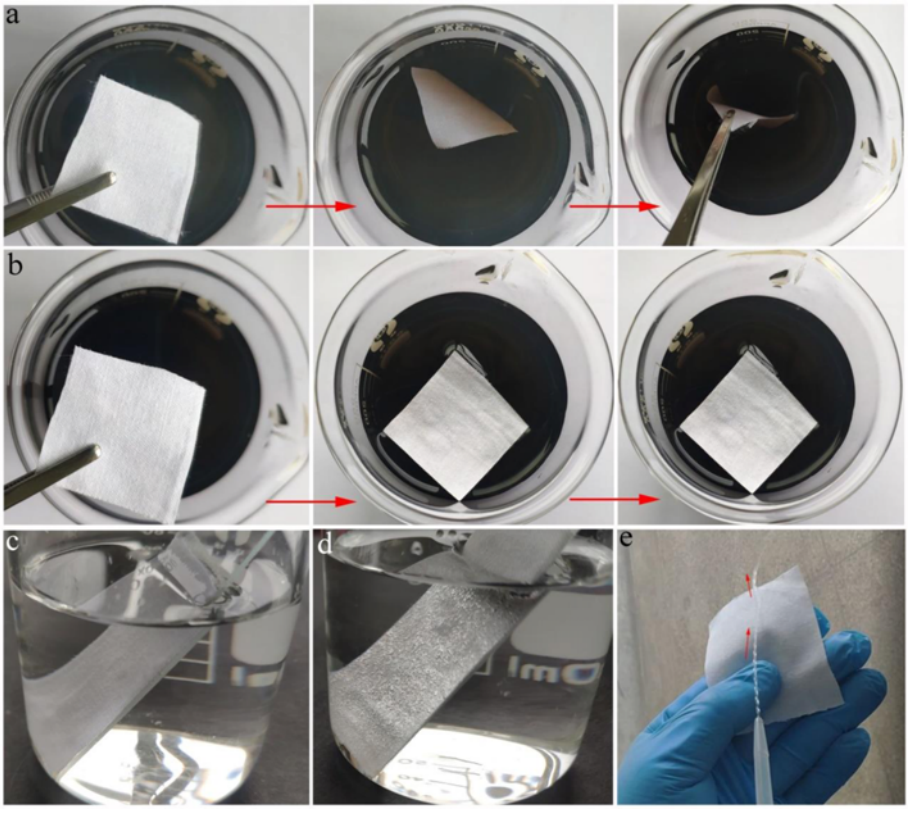

Figure 8. Image of the PF sample immersed in distilled water (a) and SF-1 sample floating on the water surface (b). Surface of the unaltered PF sample (c) and the shiny layer present on the surface of the SF-1 sample (d). Flowing water bouncing off the surface of the SF-1 sample (e).

Analysis of the Superhydrophobic Properties of the Finished Fabric

Surface roughness and energy are the decisive factors in the process of fabrication of superhydrophobic fabric surfaces. A series of qualitative and quantitative analyses were carried out to study the superhydrophobic properties of modified cotton fabric.

Figures 7a-d show the optical images of the water droplets on the fabric samples. The water droplets were wetted on the surface of the PF sample and placed on the three finished fabric samples with spherical status. The images of WCA of the fabric samples are shown in Figures 7e-h. The WCA value of the PF sample was 0.0 °, while the values of the three treated fabric samples were >150.0 °. Thus superhydrophobic surfaces were fabricated. Figures 7i and j show interesting properties of the PF and SF-1 samples. The liquid droplets encountered on a daily basis, such as the droplets of coffee, milk, and cola were all placed on the surface of SF-1 with spherical status. The droplets were wetted on the surface of the PF sample in a short time.

The optical images of PF and SF-1 placed on the water surface are shown in Figures 8a and b. The PF sample quickly drowned in water, while the SF-1 sample remained floating on the surface of water even after several minutes. Figures 8c and d show the comparison between the properties of PS and SF-1 samples as well. The surface property of the PF sample did not change in the presence of water, while a shining layer was observed in the modified surface of SF-1. When water was sprayed onto the modified surface of the SF-1 sample, it immediately bounced off. No trace of water on the SF-1 sample surface could be found (Figure 8e). These results suggested that the surface of the fabricated fabric exhibited typical superhydrophobic behavior [55,56].

Analysis of the Mechanical and Chemical Durability of the Superhydrophobic Coatings

The durability of the superhydrophobic cotton fabric is one of the important factors that must be considered while determining its ability to be used under practical application conditions. As shown in Figure 9a, the abrasion resistance of the modified cotton fabric was thoroughly analyzed. The WCA value of the SF-1 sample decreased with an increase in the number of abrasion cycles. Moreover, the SF-1 sample could withstand 1600 cycles. The WCA value recorded was >155.0 °. The WCA value of the SF-1 sample also decreased with an increase in the number of the laundering cycles (Figure 9b). Even the SF-1 sample could withstand 50 washing cycles. The surface of the treated fabric remained superhydrophobic and the WCA value recorded was 155.7 °.

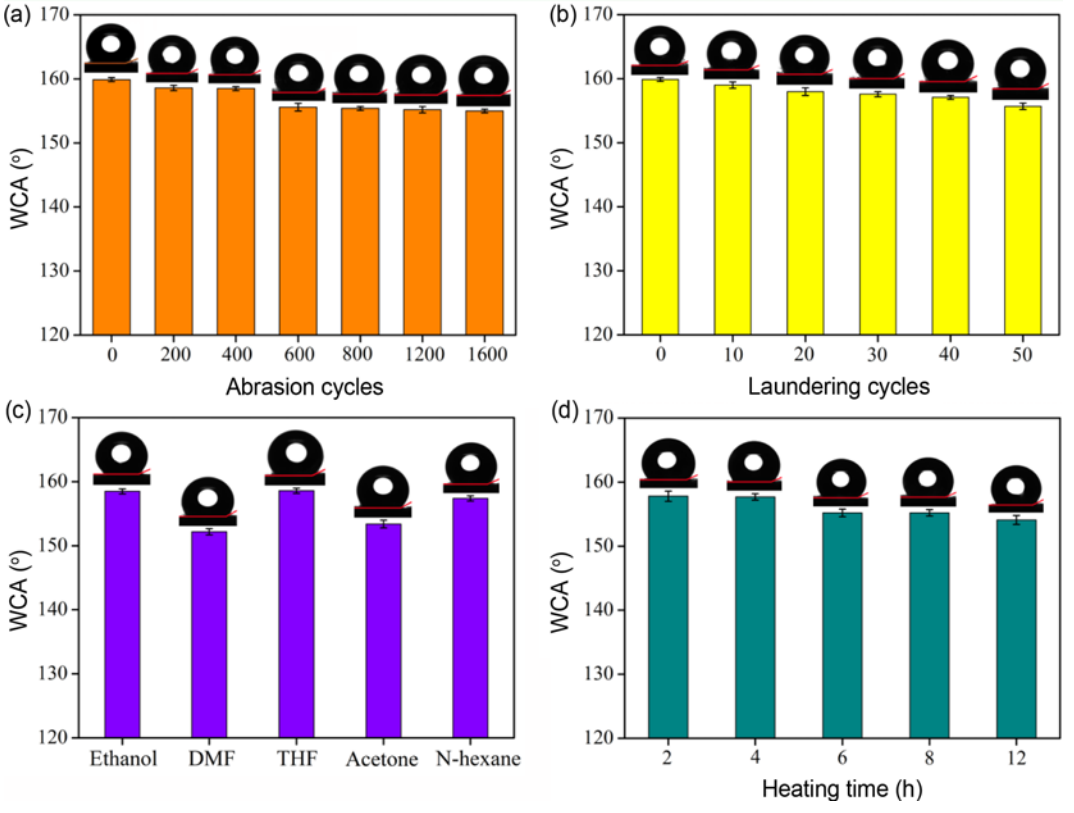

Figure 9. WCA of the SF-1 sample subjected to abrasion cycles (a), laundering cycles (b), various solvent treatment processes (c), and different heating conditions (d).

These results suggested that the SF-1 sample exhibited excellent mechanical durability.

The chemical and mechanical stability of the finished fabric should be studied. The SF-1 sample retained its superhydrophobic properties even when it was kept immersed in ethanol, DMF, THF, chloroform, and *n*-hexane for 72 h (Figure 9c). The WCA values were >152.2 °. This result proved that the modified surface of the SF-1 sample exhibited excellent chemical stability. The changes in the superhydrophobic properties of the SF-1 sample post heating (under conditions of varying times) are shown in Figure 9d. The WCA value of the SF-1 fabric remained almost constant even when the heating time was increased. This result indicated that the superhydrophobic coating on the fabric was stable even after heating (under conditions of varying time). The results indicated that the superhydrophobic coating on the surface of the cotton fiber exhibited excellent stability. Thus, these fabrics can be potentially used in industrial and household textiles.

Self-cleaning Behavior of Finished Fabrics

The fabric with excellent superhydrophobic properties exhibits excellent self-cleaning properties. Liquid pollutants and solid dust are the main sources of pollutants. Therefore, it is necessary to study the self-cleaning behavior of the fabricated fabric in the presence of these pollutants.

As shown in Figure 10, the surface of the PF sample that contained adhered methyl orange (MO) particles remained contaminated even when it was washed with a large amount of water. However, the MO particles adhered to the modified surface of the SF-1 sample could be easily removed by washing the surface with distilled water. This result proved that the modified surface of the finished cotton sample exhibited good self-cleaning properties against solid dust.

Figure 11 shows the self-cleaning effect of the fabricated fabric in the presence of liquid pollutants. The surface of the PF sample could be contaminated by immersing it in sewage. However, the modified surface of the SF-1 sample stayed clean even the fabric was immersed in sewage. This result demonstrated that the modified surface of the SF-1 sample exhibited outstanding self-cleaning properties. The above results indicated that the finished fabrics with excellent self-cleaning properties could be used to manufacture textiles used in homes.

Oil-water Separation Ability of Fabrics

The results indicated that the superhydrophobic cotton fabric possessed excellent self-cleaning properties [57]. In addition, the finished fabric can be potentially used in the field of oil-water separation. A qualitative analysis was carried out to study the oil-water separation effect of the finished cotton sample. As shown in Figure 12a, the droplets of chloroform (dyed using the oil red-o) and the droplets of water (dyed using ink) were wetted on the surface of the PF sample. However, the ink-dyed droplets of water were placed on the surface of the SF-1 sample with spherical status irrespective of whether they were wetted using oil.

Figure 12b shows the oil-water separation efficiency (η) in the presence of the chloroform/water mixture under conditions of varying separation cycles with SF-1 as the filter material. The separation efficiency of 99.4 % could be reached. Even after 50 separation cycles, the separation efficiency of the chloroform/water mixture (filter material: SF-1) was 96.6 %. Figure 12c shows the WCA values of the SF-1 sample subjected to conditions of separation cycles (chloroform/water mixture). The WCA value was >153.5 ° when the sample was subjected to 50 washing cycles in the presence of the chloroform/water mixture (filter: SF-1). The sample, under the same conditions, could be used for efficient separation in the presence of *n*-hexane/water mixtures. As shown in Figure 12d, the separation efficiency recorded under these conditions was 99.2 %. After 50

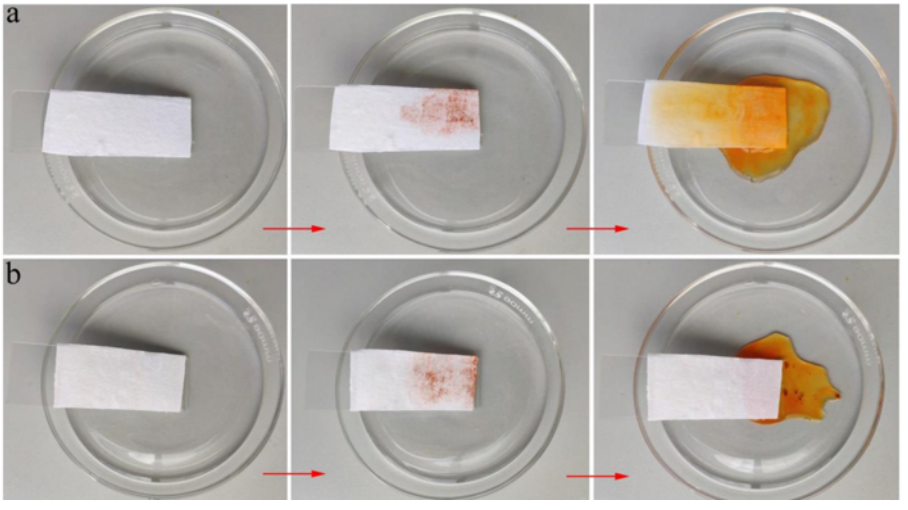

Figure 10. Self-cleaning properties in the presence of MO of the PF (a) and SF-1 (b) samples.

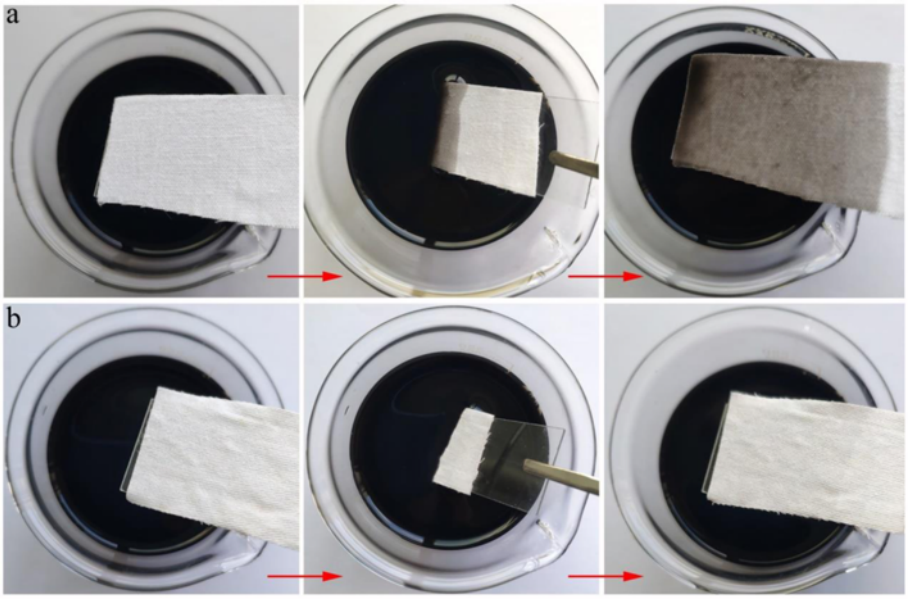

Figure 11. Self-cleaning properties of the PF (a) and SF-1 (b) samples treated with polluted water.

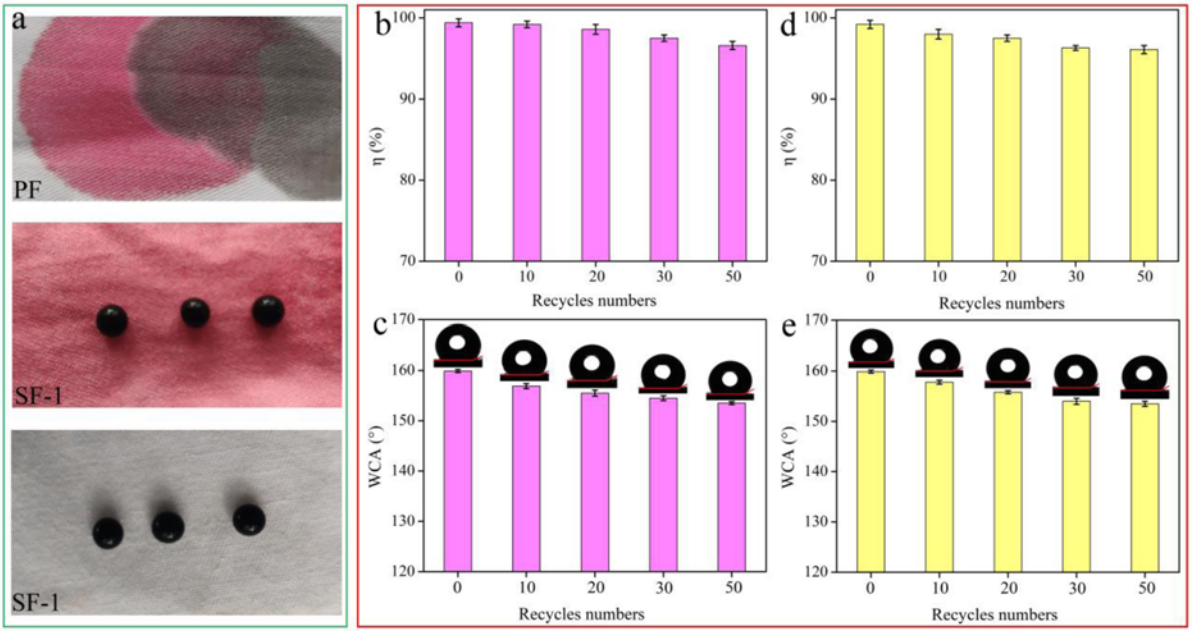

Figure 12. Water droplets (dyed by ink) and chloroform droplets (dyed by oil red-o) wetting the surface of the PF sample and the water droplets with spherical status placed on the surface of the SF-1 sample (irrespective of whether it was wetted by the chloroform droplets) (a). Separation efficiency (η) of the SF-1 sample as filter material (subjected to varying conditions of separation cycles) for the chloroform/water mixture (b) and the WCA value of the SF-1 sample that could withstand varying conditions of separation cycles (c). The separation efficiency (η) of the SF-1 sample as filter material (subjected to different conditions of separation cycles) for the *n*-hexane/water system (d), and the WCA value of the SF-1 sample that could withstand varying conditions of separation cycles (e).

separation cycles, the separation efficiency recorded was 96.1 %. Figure 12e shows the WCA value of the SF-1 sample subjected to different separation (>153.0 °). These results suggested that the obtained fabric exhibited a high level of separation efficiency. Thus, the fabricated materials can be potentially used to separate oil from water.

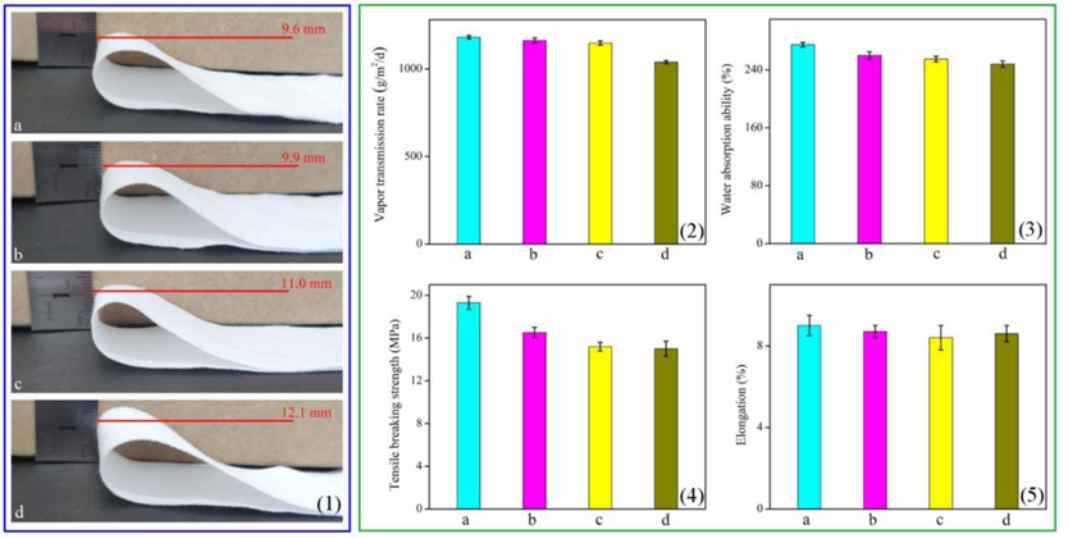

Figure 13. Flexibility (1), water vapor permeability (2), water absorption (3), tensile strength (4), and elongation at break (5) of the PF (a), SF-1 (b), SF-2 (c), and SF-3 (d) samples.

Analysis of the Inherent Properties of the Finished Fabric

It is important to analyze the inherent properties of functional fabrics [58-60]. The water absorption ability, water vapor permeability, flexibility, and mechanical strength of modified fabric are the key factors that determine if the fabrics can be used in industries and at home. Figure 13 shows the inherent properties of PF and the modified fabrics. The loop height of the PF fabric was 9.6 mm, while the loop heights of SF-1, SF-2, and SF-3 were 9.9 mm, 11.0, and 12.1 mm, respectively (Figure 13(1)). The lower the loop height, the better the flexibility of the fabric. Compared with the PF sample, the loop heights of the modified fabrics were slightly higher (within the acceptable range). Figure 13(2) shows the water vapor permeabilities of the PF, SF-1, SF-2, and SF-3 samples. The water vapor permeabilities of SF-1 and SF-2 were comparable to the water vapor permeability of the PF sample, while the water vapor permeability of SF-3 was lesser than that of the PF sample (percentage of reduction: ≤12.0 %). The trend in the water absorption abilities of SF-1, SF-2, and SF-3 was similar to the trend observed for the water vapor permeabilities (Figure 13(3)). The etching treatment resulted in a significant reduction in the mechanical strength of the fabric. The tensile strengths of PF, SF-1, SF-2, and SF-3 are shown in Figure 13(4). Compared to the tensile strength of the PF sample, the tensile strengths of SF-1, SF-2, and SF-3 were lesser. The degree of reduction degree was ≤ 22.2 %. Figure 13(5) shows the elongation at break of the PF, SF-1, SF-2, and SF-3 samples. In general, the elongation at break values of the SF-1, SF-2, and SF-3 samples were similar to that of the PF sample. These results suggested that a combination of the etching method and mist polymerization technique did not significantly affect the properties of the superhydrophobic fabrics.

Conclusion

Durable superhydrophobic cotton fabric was successfully prepared using a combination of the etching and mist polymerization techniques. The coatings endow the modified surface of the finished fabric with excellent superhydrophobic properties. The WCA value of the modified surface was 159.9 °. The modified surface of the fabricated fabric exhibits outstanding mechanical and chemical stabilities. Even after 1600 abrasion treatments or 50 washing cycles, the WCA value was higher than 155.0 °. The superhydrophobic properties of the finished fabric were retained to a large extent even when the fabrics were treated with various solvents (e.g., ethanol and DMF) for 72 h. The finished fabric with excellent superhydrophobic properties also exhibited good self-cleaning properties in the presence of solid dust and liquid pollutants. In addition, the finished fabric also exhibited excellent oil-water separation properties. The oil-water separation efficiencies of the treated fabric for chloroform/water and *n*-hexane/water systems were 99.4 % and 99.2 %, respectively. Even after 50 repetitions of oil-water separation cycles, the separation efficiency of the finished fabric for those mixtures was higher than 96.0%. The WCA values of the finished cotton fabric that was subjected to 50 separation cycles for chloroform/water and *n*-hexane/water systems were higher than 153.0 °. The desired properties, such as flexibility and mechanical strength of the cotton fabrics, did not significantly alter post treatment. Therefore, we believe that the prepared fabric can

be potentially used to manufacture fabrics that can be used in industries and at homes.

Acknowledgments

This work was financially supported by the Open Project Program of Anhui Engineering and Technology Research Center of Textile, Anhui Province College of Anhui Province College Key Laboratory of Textile Fabrics (No. 2021AETKL18) and the Starting Research Fund from the Anhui Polytechnic University (No. S022021008).

Electronic Supplementary Material (ESM) The online version of this article (doi: 10.1007/s12221-022-4992-4) contains supplementary material, which is available to authorized users.

References

1. H. Wang, R. Kumar, and H. Memon, *Coatings*, **10**, 943 (2020).
2. N. Zhang, Y. Qi, Y. Zhang, J. Luo, P. Cui, and W. Jiang, *Ind. Eng. Chem. Res.*, **59**, 14546 (2020).
3. J. Hou, Y. Yang, D. G. Yu, Z. Chen, K. Wang, Y. Liu, and G. R. Williams, *Chem. Eng. J.*, **411**, 128474 (2021).
4. H. Wang and H. Memon, "Cotton Science and Processing Technology: Gene, Ginning, Garment and Green Recycling", Springer Nature, 2020.
5. S. N. Saleh, M. M. Khaffaga, N. M. Ali, M. S. Hassan, A. W. M. El-Naggar, and A. G. M. Rabie, *Int. J. Biolo. Macromol.*, **183**, 23 (2021).
6. A. Errokh, W. Cheikhrouhou, A. M. Ferraria, A. M. B. do Rego, and S. Boufi, *Colloid. Surface. B*, **200**, 111600 (2021).
7. M. Verma, N. Gahlot, S. S. J. Singh, and N. M. Rose, *Carbohydr. Polym.*, **257**, 117612 (2021).
8. N. Čuk, M. Šala, and M. Gorjanc, *Cellulose*, **28**, 3215 (2021).
9. H. Barani and B. Mahltig, *Cellulose*, **27**, 9105 (2020).
10. S. Wang, X. Du, Y. Luo, S. Lin, M. Zhou, Z. Du, and H. Wang, *Chem. Eng. J.*, **408**, 127363 (2021).
11. V. Trovato, E. Teblum, Y. Kostikov, A. Pedrana, V. Re, G. D. Nessim, and G. Rosace, *J. Colloid Interf. Sci.*, **586**, 120 (2021).
12. J. Ou, F. Wang, W. Li, M. Yan, and A. Amirfazli, *Prog. Org. Coat.*, **146**, 105700 (2020).
13. D. Cheng, Y. Zhang, X. Bai, Y. Liu, Z. Deng, J. Wu, and X. Wang, *Cellulose*, **27**, 5421 (2020).
14. P. Chauhan, A. Kumar, and B. Bhushan, *J. Colloid Interf. Sci.*, **535**, 66 (2019).
15. H. Liu, L. Yang, Y. Zhan, J. Lan, J. Shang, M. Zhou, and S. Lin, *Cellulose*, **28**, 1715 (2021).
16. Q. Shang, C. Liu, J. Chen, X. Yang, Y. Hu, L. Hu, and X. Ren, *ACS Sustain. Chem. Eng.*, **8**, 7423 (2020).
17. S. P. Dalawai, M. A. S. Aly, S. S. Latthe, R. Xing, R. S. Sutar, S. Nagappan, and S. Liu, *Prog. Org. Coat.*, **138**, 105381 (2020).
18. T. C. Lin and D. J. Lee, *Cellulose*, **28**, 4575 (2021).
19. M. Yang, W. Liu, C. Jiang, S. He, Y. Xie, and Z. Wang, *Carbohydr. Polym.*, **197**, 75 (2018).
20. J. Ren, F. Tao, L. Liu, X. Wang, and Y. Cui, *Carbohydr. Polym.*, **232**, 115807 (2020).
21. T. He, H. Zhao, Y. Liu, C. Zhao, L. Wang, H. Wang, and H. Wang, *Colloid. Surface. A*, **585**, 124080 (2020).
22. N. Ahmad, S. Kamal, Z. A. Raza, S. Abid, and M. Zeshan, *Fiber. Polym.,* **21**, 1039 (2020).
23. G. D. Patil, A. H. Patil, S. A. Jadhav, C. R. Patil, and P. S. Patil, *Mater. Lett.*, **255**, 126562 (2019).
24. Y. He, M. Wan, Z. Wang, X. Zhang, Y. Zhao, and L. Sun, *Surf. Coat. Tech.*, **378**, 125079 (2019).
25. Z. Du, P. Ding, X. Tai, Z. Pan, and H. Yang, *Langmuir*, **34**, 6922 (2018).
26. S. K. Lahiri, P. Zhang, C. Zhang, and L. Liu, *ACS Appl. Mater. Interfaces*, **11**, 10262 (2019).
27. N. Jannatun, A. Taraqqi-A-Kamal, R. Rehman, J. Kuker, and S. K. Lahiri, *Eur. Polym. J.*, **134**, 109836 (2020).
28. D. Li and Z. Guo, *Appl. Surf. Sci.*, **426**, 271 (2017).
29. Q. Zhou, B. Yan, T. Xing, and G. Chen, *Carbohydr. Polym.*, **203**, 1 (2019).
30. Q. Zhou, G. Chen, and T. Xing, *Cellulose*, **25**, 1513 (2018).
31. C. H. Xue, L. L. Zhao, X. J. Guo, Z. Y. Ji, Y. Wu, S. T. Jia, and Q. F. An, *Chem. Eng. J.*, **396**, 125231 (2020).
32. M. Wang, M. Peng, Y. X. Weng, Y. D. Li, and J. B. Zeng, *Cellulose*, **26**, 8121 (2019).
33. Q. Xu, L. Wang, F. Fu, and X. Liu, *Prog. Org. Coat.*, **148**, 105884 (2020).
34. P. Nguyen-Tri, F. Altiparmak, N. Nguyen, L. Tuduri, C. M. Ouellet-Plamondon, and R. E. Prud'homme, *ACS Omega*, **4**, 7829 (2019).
35. Q. Y. Cheng, X. L. Zhao, Y. X. Weng, Y. D. Li, and J. B. Zeng, *ACS Sustain. Chem. Eng.*, **7**, 15696 (2019).
36. Q. Y. Cheng, X. L. Zhao, Y. D. Li, Y. X. Weng, and J. B. Zeng, *Int. J. Biol. Macromol.*, **140**, 1175 (2019).
37. Y. Cheng, T. Zhu, S. Li, J. Huang, J. Mao, H. Yang, and Y. Lai, *Chem. Eng. J.*, **355**, 290 (2019).
38. G. Xi, J. Wang, G. Luo, Y. Zhu, W. Fan, M. Huang, and X. Liu, *Cellulose*, **23**, 915 (2016).
39. Q. Xu, L. Xie, H. Diao, F. Li, Y. Zhang, F. Fu, and X. Liu, *Carbohydr. Polym.*, **177**, 187 (2017).
40. Q. Xu, X. Ke, D. Cai, Y. Zhang, F. Fu, T. Endo, and X. Liu, *Cellulose*, **25**, 2129 (2018).
41. X. W. Cheng, R. C. Tang, J. P. Guan, and S. Q. Zhou, *Prog. Org. Coat.*, **141**, 105539 (2020).
42. D. Wang, L. Zhong, C. Zhang, S. Li, P. Tian, F. Zhang, and G. Zhang, *Cellulose*, **26**, 2123 (2019).
43. Y. Yang, X. Bao, Q. Wang, P. Wang, M. Zhou, and Y. Yu, *Cellulose*, **28**, 1795 (2021).
44. L. Wang, X. Wen, X. Zhang, S. Yuan, Q. Xu, F. Fu, and X.

Liu, *Cellulose*, **28**, 5867 (2021).
45. Z. Wang, A. Yang, X. Tan, Y. Tu, S. Sabin, P. Xiang, M. Wang, R. Guo, and X. Chen, *Colloid. Surface A.*, **601**, 124998 (2020).
46. W. Li, X. Tan, J. Zhu, P. Xiang, T. Xiao, L. Tian, A. Yang, M. Wang, and X. Chen, *Mater. Today Energy*, **12**, 348 (2019).
47. W. Wang, J. Wang, X. Wang, S. Wang, X. Liu, P. Qi, and X. Gu, *Prog. Org. Coat.*, **149**, 105930 (2020).
48. S. Zhong, L. Yi, J. Zhang, T. Xu, L. Xu, X. Zhang, and Y. Cai, *Chem. Eng. J.*, **407**, 127104 (2021).
49. P. Li, B. Wang, Y. Y. Liu, Y. J. Xu, Z. M. Jiang, C. H. Dong, and P. Zhu, *Carbohydr. Polym.*, **237**, 116173 (2020).
50. L. Rong, H. Liu, B. Wang, Z. Mao, H. Xu, L. Zhang, and X. Sui, *Carbohydr. Polym.*, **211**, 173 (2019).
51. T. Zhou, H. Xu, L. Cai, and J. Wang, *Appl. Surf. Sci.*, **507**, 145175 (2020).
52. Y. Yang, Z. Guo, W. Huang, S. Zhang, J. Huang, H. Yang, and S. Gu, *Appl. Surf. Sci.*, **503**, 144079 (2020).
53. Z. Jiang, H. Li, Y. He, Y. Liu, C. Dong, and P. Zhu, *Appl. Surf. Sci.*, **479**, 765 (2019).
54. C. Ling and L. Guo, *Carbohydr. Polym.*, **230**, 115648 (2020).
55. K. Zhu, J. Zhang, H. Zhang, H. Tan, W. Zhang, Y. Liu, and Q. Zhang, *Chem. Eng. J.*, **351**, 569 (2018).
56. K. Hou, Y. Zeng, C. Zhou, J. Chen, X. Wen, S. Xu, and P. Pi, *Chem. Eng. J.*, **332**, 150 (2018).
57. X. Tan, Y. Wang, Z. Huang, S. Sabin, T. Xiao, L. Jiang, and X. Chen, *Adv. Mater. Interfaces*, **8**, 2002209 (2021).
58. J. Zhou, X. Hu, Y. Zhu, H. Lyu, L. Zhang, F. Fu, and X. Liu, *Cellulose*, **26**, 9323 (2019).
59. D. Cai, J. Zhou, P. Duan, G. Luo, Y. Zhang, F. Fu, and X. Liu, *Cellulose*, **25**, 7355 (2018).
60. Q. Xu, W. Zheng, P. Duan, J. Chen, Y. Zhang, F. Fu, and X. Liu, *Carbohydr. Polym.*, **204**, 42 (2019).